Ore Geology Reviews 184 (2025) 106715

Contents lists available at ScienceDirect

Ore Geology Reviews

journal homepage: www.elsevier.com/locate/oregeorev

Enhanced solubility of gold in crude oil at high temperatures: new insights into ore genesis

Zhiyong Ni [a,b,*], Hengwang Cui [a,b], Huan Chen [c], Kai Shi [a,b], Weng Zhang [a,b], Ganggang Shao [a,b]

[a] State Key Laboratory of Petroleum Resources and Engineering, China University of Petroleum, Beijing 102249, China
[b] College of Geosciences, China University of Petroleum, Beijing 102249, China
[c] School of Civil and Resource Engineering, University of Science and Technology Beijing, Beijing 100083, China

ARTICLE INFO

Keywords:
Gold
Crude Oil
Ore-forming Fluid
Metal Transport

ABSTRACT

Gold's exceptional conductivity and corrosion resistance make it indispensable in various industries, yet its transport and deposition mechanisms remain a subject of exploration. While hydrothermal fluids are traditionally considered the primary medium for gold mobilization, recent evidence suggests hydrocarbons could also transport metals under specific conditions. This study investigates the solubility of gold in crude oil with varying compositions at temperatures up to 250 °C, focusing on the role of sulfur (S) content and Total Acid Number (TAN). Crude oils from the Bohai Bay Basin, China, were exposed to gold wires for durations of up to 30 days in a quartz tube and titanium alloy tube setup. Results reveal that gold solubility increases with temperature and time, with maximum concentrations observed at 250 °C. The highest solubility (19.8 ppm) was observed in the oil sample with the highest sulfur (S) and Total Acid Number (TAN) content. Furthermore, X-ray Photoelectron Spectroscopy (XPS) analysis indicates that gold (Au) exhibits a strong affinity for carbon-, oxygen-, and sulfur-containing compounds in crude oil, suggesting the formation of thiol or organic acetate complexes. Post-experiment SEM analysis revealed significant surface erosion of gold wires, supporting the hypothesis of enhanced gold dissolution in hydrocarbons at elevated temperatures. These findings challenge conventional ore genesis models by highlighting hydrocarbons as a potential medium for metal transport in organic-rich and petroleum-bearing environments, offering new perspectives for understanding hydrocarbon-driven gold mineralization.

1. Introduction

Gold's exceptional conductivity and resistance to corrosion make it vital for numerous applications in high-tech industries, including electronics, aerospace, and medical devices. These properties, combined with its rarity, have driven extensive exploration and study of gold deposits globally. Most of the world's gold production comes from lode deposits, where gold is transported and concentrated by hydrothermal fluids within the Earth's crust (Chen et al., 2007; Groves, 1993; Goldfarb and Pitcairn, 2023). Such deposits have been widely studied and are known to form through complex geological processes involving the migration of gold-bearing hydrothermal fluids along fractures and faults (Chen et al., 2007; Groves et al., 2020; Kerrich et al., 2005). These fluids facilitate gold transport by stabilizing gold complexes, often as thio-complexes, under specific pressure–temperature conditions (Gibert et al., 1998; Helgeson and Garrels, 1968; Li et al., 2022; Tomkins, 2013). While hydrothermal models remain the cornerstone of gold mineralization studies, emerging research suggests that hydrocarbons might also act as efficient metal-transporting agents (Crede et al., 2019; Emsbo et al., 2009; Gaboury, 2013, 2021; Hu and Plet, 2022; Migdisov et al., 2017; Williams-Jones and Migdisov, 2006). Hydrocarbons, particularly crude oil, exhibit unique physicochemical properties that allow them to dissolve metals under suitable conditions, especially within the temperature range of the "oil window" (80–160 °C; Peters et al., 2004). This unconventional concept challenges traditional views and is supported by growing evidence that links hydrocarbons to gold mineralization in several major deposits, including Carlin-type gold deposits in Nevada, the Youjiang Basin in China, and the Witwatersrand Au-U deposits in South Africa (Fuchs et al., 2021; Gu et al., 2010; Hulen and Collister, 1999; Williams-Jones and Migdisov, 2006). In these regions, gold

* Corresponding author at: State Key Laboratory of Petroleum Resources and Engineering, China University of Petroleum, Beijing 102249, China.
E-mail address: nizhy@cup.edu.cn (Z. Ni).

https://doi.org/10.1016/j.oregeorev.2025.106715
Received 6 January 2025; Received in revised form 8 April 2025; Accepted 4 June 2025
Available online 6 June 2025

deposits and hydrocarbon reservoirs exhibit a close spatial association. For example, northeastern Nevada in the United States is a globally recognized district for Carlin-type gold deposits and also hosts numerous oil and gas fields (Hulen et al., 1998). Similarly, the Youjiang Basin, located at the intersection of Yunnan, Guizhou, and Guangxi provinces in China, is characterized by widespread Carlin and Carlin-like gold deposits. This region is also notable for its abundance of paleo-oil reservoirs and residual hydrocarbon accumulations, making it a strategic target for marine hydrocarbon exploration in southern China (Wang et al., 2002). Furthermore, in eastern Guizhou, the Tongren–Wanshan and the Kaili–Majiang–Danzhai paleo-oil reservoir belt host more than a dozen low-temperature hydrothermal deposits of Hg, Sb, As, and Au have been identified (Hu et al., 2007). In the Witwatersrand Basin of South Africa, the presence of carbonaceous matter in gold- and uranium-bearing conglomerates is one of the most intriguing and debated aspects of deposit formation. This organic material is of particular interest in mining, as it typically coincides with high concentrations of both gold and uranium. In some cases, isolated carbonaceous material has been reported to contain up to 4.7 wt% gold and 11.5 wt% uranium (Drennan and Robb, 2006). A key feature of ore-hosting rocks in Carlin-type gold deposits is their enrichment in various forms of organic matter (Arehart, 1996). Organic components have been implicated in the mineralization process across all Carlin-type deposits. In the Yankee Basin of northeastern Nevada, for instance liquid hydrocarbons and petroleum-bearing fluid inclusions have been directly observed. Thermometric analyses show that these inclusions were trapped at temperatures below 150 °C (Hulen and Collister, 1999), within the typical oil window range of 80–160 °C. Likewise, the Shuiyindong gold deposit in the Youjiang Basin features ore enriched in organic matter and bitumen. Fluid inclusions containing CH_4, CO_2, and N_2 have been identified in auriferous quartz veins, with carbon and nitrogen likely derived from organic matter decomposition (Su, 2002). The frequent coexistence of oil accumulations and hydrothermal mineral deposits, both at macroscopic and microscopic scales, may be attributed to their shared geological processes. These include the generation and migration of hydrothermal fluids and the subsequent enrichment of metals in mineralized zones (Chen et al., 2001, 2007; Giordano, 1994; Kesler et al., 1994). Complex interactions between organic and inorganic substances in these fluids have been observed during the evolution of sedimentary basins and are frequently associated with the formation of mineral deposits (Broadbent et al., 1998; Disnar and Sureau, 1990; Etminan and Hoffmann, 1989; Jaraula et al., 2015; Mossman, 1999). Previous studies have primarily explored either the capacity of oilfield brine to transport metals or the role of organic substances in facilitating the precipitation of metals from fluids during mineral deposit formation (Anderson, 2008; Herazo et al., 2020; Sanz-Robinson and Williams-Jones, 2019; Sun and Püttmann, 2000). However, the direct involvement of oil in metal migration and precipitation processes remains a subject of debate.

Experimental investigations have demonstrated that organic-rich fluids can dissolve various metals, including gold, antimony, nickel, palladium, and zinc, providing a plausible mechanism for metal transport across sedimentary basins and petroleum reservoirs (Migdisov et al., 2017; Sanz-Robinson et al., 2020; Sanz-Robinson and Williams-Jones, 2019; Sanz-Robinson and Williams-Jones, 2020; Su et al., 2024). For example, William-Jones and Migdisov (2006) reported gold solubility in crude oil reaching up to 14 ppm at 200 °C. However, subsequent studies observed significantly lower solubility values, such as the 50 ppb reported by Migdisov et al. (2017), highlighting inconsistencies that warrant further investigation. By comparison, the solubility of gold in hydrothermal fluids at 350 °C is approximately 52 ± 8 ppb (Gibert et al., 1998). These variations underscore the need to better understand gold's behavior in non-aqueous environments, particularly in the context of crude oil (Migdisov et al., 2017; William-Jones and Migdisov, 2006). Gold transport in hydrothermal fluids is well understood to occur predominantly in the aurous state. Despite low concentrations, typically around 20 ppb, such fluids can form economically significant gold deposits over geological timescales (Helgeson and Garrels, 1968). Extending this understanding to crude oil systems involves examining whether crude oil's capacity to dissolve and transport gold is comparable to that of hydrothermal systems. The potential for hydrocarbons to dissolve gold and other metals at elevated temperatures and pressures is increasingly being recognized as a critical factor in developing new models of ore genesis.

This study aims to reevaluate the solubility of gold in crude oil under controlled experimental conditions, exploring a temperature range up to 250 °C. Particular attention is given to the role of crude oil composition, including sulfur content and Total Acid Number (TAN), as potential factors influencing gold dissolution. By systematically comparing gold solubility in crude oil to established data on hydrothermal fluids, this research seeks to refine our understanding of unconventional metal transport mechanisms and their implications for ore-forming processes.

2. Methods

The experiment was conducted using a sealed quartz tube and a titanium alloy autoclave setup. The materials used included gold wire (≥99.9 %, 0.3 mm diameter), quartz tubes (6 mm outer diameter, 4 mm inner diameter, 10 cm length), quartz rods (1 mm diameter, 5 cm length), and titanium alloy autoclaves. Prior to the experiment, quartz tubes and rods were cleaned with trace-metal grade nitric acid (~75 % HNO_3) for 24 h, neutralized with ultrapure water, and dried at 100 °C for 2 h. A diamond grinding needle was used to create a circular groove 0.8 cm from one end of the quartz rod to secure the gold wire. Gold wire was measured and cut to 4 mm, wound into the groove, and fixed in place. The prepared quartz rod, with the gold wire end facing down, was placed into a quartz tube sealed at one end. Approximately 0.2 g of crude oil was weighed into the quartz tube, which was then sealed with a hydroxygen flame welding torch. The sealed quartz tube was placed in an autoclave, and distilled water was added to the autoclave to balance internal and external pressures. The muffle furnace was preheated to the target temperature (150 °C, 200 °C, or 250 °C), and the autoclaves were placed inside, arranged in four rows of three, corresponding to heating durations of 30, 15, 10, and 5 days. After heating, the autoclaves were removed while still hot, inverted to separate the gold wire from the crude oil, and placed in a beaker filled with room-temperature tap water to cool, completing the quenching process (Fig. 1).

The autoclave was opened, and the quartz tube containing the crude oil was removed. The quartz tube was cut into two 5 cm sections using a file. The gold wire was extracted, and the openings of the quartz tubes were sealed with quartz wool to prevent crude oil leakage during calcination. The two quartz tube sections were placed into a ceramic crucible and ashed in a muffle furnace at 550 °C for 24 h. After calcination, the quartz wool was removed, and the tubes were transferred to a 50 ml centrifuge tube. Aqua regia (2 ml, consisting of 500 μl HCl and 1500 μl HNO_3) was added to the centrifuge tube, which was then diluted to 50 ml with deionized water and shaken thoroughly. The tube was left to stand for 24 h, and the solution was drawn out and filtered using a 0.45 μm hydrophilic filter membrane into a 10 ml centrifuge tube. This process was repeated until 10 ml of filtered solution was obtained.

For analysis, 1 ml of the filtered solution was diluted to 10 ml with 1 % HNO_3. A NexION 350X inductively coupled plasma–mass spectrometry (ICP–MS) system was used for gold analysis. The system featured a three-cone interface (sampling, interceptor, over-interceptor cones), a triple four-pole ion deflector, and universal cell technology with a wide linear range. Rhodium (Rh) was used as an internal standard. Working parameters were automatically optimized, with a transmission power of 1250 W, a carrier gas flow rate of 0.82 L/min, a peristaltic pump speed of 20 rpm, and scanning repeated 20 times with triplicate sample analyses. Gold standard solutions were manually prepared at concentrations of 0.5 ppb, 2 ppb, 10 ppb, and 40 ppb. The test results produced a linear regression curve for the gold standard solution, with $R^2 > 0.99995$.

The Total Acid Number (TAN) of crude oil samples was determined

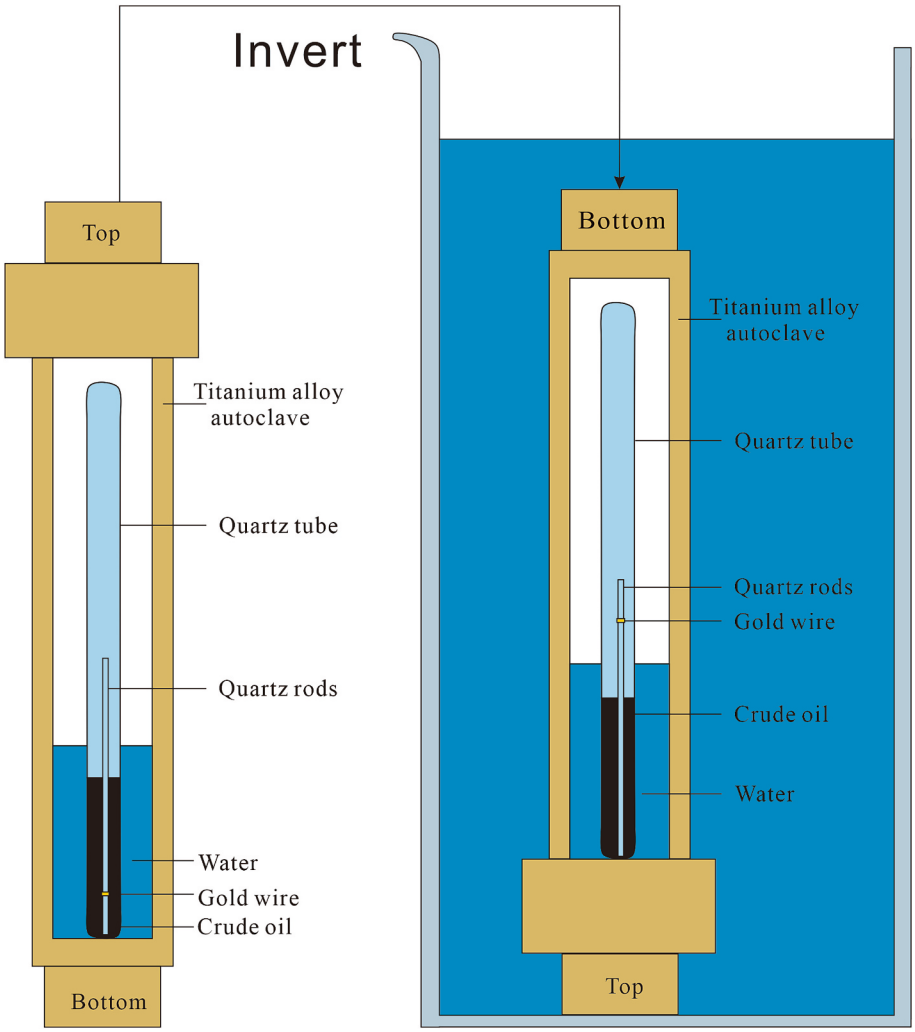

Fig. 1. Schematic Diagram of the Experimental Setup.

through acid-base titration in accordance with the GB/T 264 PRC National Standard at the China University of Petroleum. Crude oil samples (2 g) were dissolved in 25 mL of neutral ethanol in a conical flask, followed by the addition of 25 mL of anhydrous ether. A blank sample, containing 25 mL of ethanol and 25 mL of ether, was prepared for comparison. To each mixture, 1 mL of phenolphthalein solution was added, and titration was carried out using 0.1 mol/L KOH until a pink endpoint was observed. The Total Acid Number (TAN) was calculated using the formula: $TAN = (V_1 - V_2) \times C \times 56.1$, where: V_1 is the volume of KOH used for the sample titration (mL), V_2 is the volume of KOH used for the blank titration (mL), and C is the concentration of the KOH solution (mol/L).

The gold wires obtained after the solubility experiments were analyzed using X-ray photoelectron spectroscopy (XPS, ThermoFisher, USA) at China University of Petroleum. Measurements were carried out with Al Kα radiation over a spectral range of 0–1100 eV, employing a resolution of 20 eV, a step size of 0.1 eV, and a spot diameter of 300 μm. Surface etching was performed using X-ray exposure for 0, 30, and 60 s to examine depth-dependent variations in the elemental composition of carbon (C), oxygen (O), sulfur (S), and gold (Au). Data visualization and graphing were conducted using ORIGIN software.

The gold wires, both before and after the solubility experiments, were observed and compositionally analyzed using a Phenom XL benchtop scanning electron microscope equipped with an energy dispersive spectrometer (SEM-EDS) at an accelerating potential of 15 kV.

3. Results

In this study, gold wires were immersed in three types of crude oils (designated as A, B, and C) sourced from the Bohai Bay Basin—one of China's most petroleum-rich regions, contributing nearly 30 % of the country's total oil production (Hao et al., 2011). The oils display diverse compositions and physical properties. Oil A possesses the highest sulfur content (0.36 %) and Total Acid Number (TAN, 1.52 mg KOH/g), Oil B exhibits the lowest values (S, 0.10 %; TAN, 0.82 mg KOH/g), and Oil C falls in between (S, 0.25 %; TAN, 1.22 mg KOH/g). Their densities range from 0.863 to 0.893 g/cm3, and dynamic viscosities vary from 11.3 to 41.0 mPa·s. Initial measurements revealed gold concentrations between 17 and 32 ppb (Table 1); notably, Oil B showed the highest native gold content despite its lower S and TAN levels, suggesting that factors such as the geological origin and mineralization history of the source rock may also play a role.

Experimental data (Table 2) indicate that gold solubility in all three oils increases continuously with time. For example, at 250 °C, the gold concentration in Oil A rises from approximately 4.6 ppm after 5 days to 19.8 ppm after 30 days, implying that equilibrium has not yet been reached. Similar time-dependent trends are observed in Oils B and C, although their absolute solubility values are consistently lower than those in Oil A. Additionally, gold solubility significantly increases with temperature. Fig. 2 clearly shows that at 150 °C, 200 °C, and 250 °C, there is a positive correlation between temperature and gold solubility. While Oil A's solubility curve is notably higher overall, its initial gold

Table 1
Composition and properties of the three crude oils (A, B, and C) used in the experiments.

Sample No.	Well No.	Production Formation	Depth (m)	Density (g/cm^3)	Viscosity (mPa·s)	S content (%)	TAN (mg KOH/g)	Au content (ppb)
A	S8-29	Es^2	1854–1859	0.887	21.5	0.36	1.52	29
B	L76-3	Es^4	2069–2094	0.893	41.0	0.10	0.82	32
C	S70-X5	Es^2	2349–2374	0.863	11.3	0.25	1.22	18

Es^2: the second member of the Shahejie Formation from the Eocene epoch.
Es^4: the fourth member of the Shahejie Formation from the Eocene epoch.

Table 2
The experimentally determined solubility of Au (ppm) in oils A, B, and C at 150 °C, 200 °C, and 250 °C over durations of 5, 10, 15, and 30 days.

Experiment temperature: 150 °C				
Experiment Duration (Days)	**5**	**10**	**15**	**30**
Oil A	2.7	5.7	7.8	10.9
Oil B	2.3	2.9	4.8	6.9
Oil C	4.4	4.9	6.6	8.3
Experiment temperature: 200 °C				
Experiment Duration (Days)	**5**	**10**	**15**	**30**
Oil A	3.1	7.6	12.0	15.7
Oil B	2.7	5.1	6.1	8.9
Oil C	3.2	5.7	8.7	11.6
Experiment temperature: 250 °C				
Experiment Duration (Days)	**5**	**10**	**15**	**30**
Oil A	4.6	6.8	10.8	19.8
Oil B	2.0	4.0	6.1	9.6
Oil C	2.4	6.1	9.2	13.6

solubility is lower than that of the other oils (Fig. 2). Scanning Electron Microscope (SEM) analyses of the post-reaction gold wires (Fig. 3) further confirm the dissolution process, revealing extensive surface erosion and numerous dissolution pits that were absent on pristine wires. The density and size of these pits vary among the oils: Oil A produces the most pronounced pitting, followed by Oil C, whereas Oil B results in a comparatively smoother surface. These observations underscore the significant role of sulfur and acid content in facilitating gold dissolution.

To further elucidate the process, X-ray Photoelectron Spectroscopy (XPS) was conducted on the gold wires after the solubility experiments. Spectra for Au, C, O, and S were recorded at etching times of 0, 30, and 60 s (Fig. 4). The peaks corresponding to Au ($4f_{5/2}$ at 87 eV and $4f_{7/2}$ at 84 eV), Carbon (1 s at 283 eV), Oxygen (1 s at 530 eV), and Sulfur ($4p_{3/2}$ at 162 eV) were clearly identified, with their peak areas increasing with etching time. Furthermore, the S ($4\ p_{3/2}$) spectra shifted toward an unbound thiol peak at 163 eV (depicted in pink), while sulfur peaks bound to gold were observed at 162 eV (blue) and 160 eV (green) (Fig. 5).

4. Discussion

The continuous increase in gold solubility over the 5–30 day period indicates that the reaction between gold and crude oil had not reached equilibrium during the experiments. Notably, the measured gold solubility in our study is significantly higher than that reported in previous works (William-Jones and Migdisov, 2006; Migdisov et al., 2017). These discrepancies likely arise from differences in experimental methodologies, including reaction durations and system configurations. For example, Migdisov et al. (2017) conducted experiments over shorter periods (5–10 days), which may have been insufficient for the gold dissolution process to fully develop. In contrast, our experiments were performed over longer durations, and even at equivalent time intervals, the gold solubility in our crude oil (at least 2 ppm) was markedly higher than the previous maximum of no more than 50 ppb. We attribute this

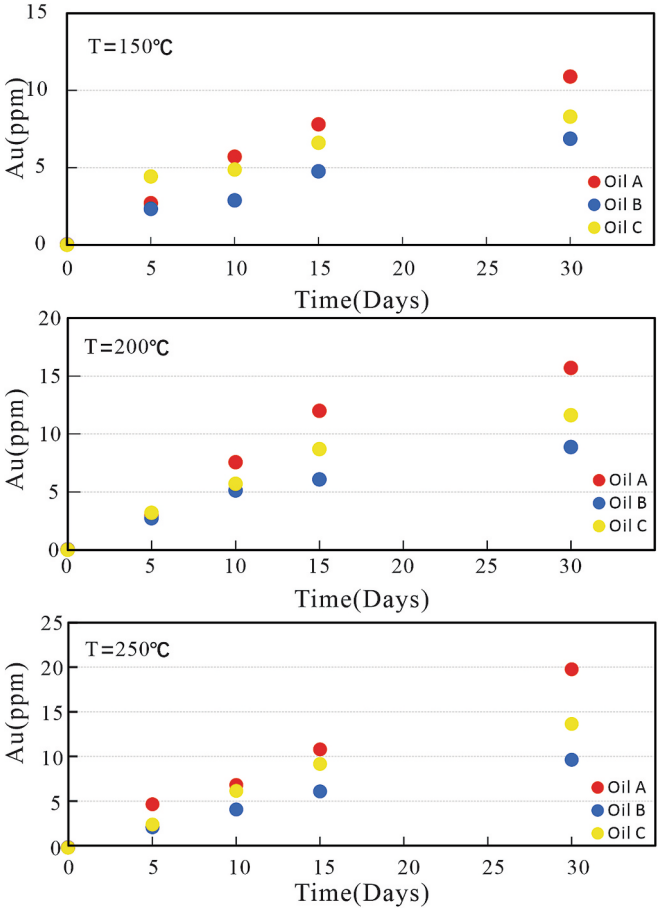

Fig. 2. Concentration of gold in crude oils A, B, and C at varying temperatures as a function of experiment duration.

primarily to our experimental method, where the autoclaves were inverted prior to quenching, thereby separating the gold wires from the crude oil. This approach prevented the redeposition of gold during the cooling phase, thereby enhancing the accuracy of the solubility measurements and revealing a greater capacity of crude oil to dissolve gold.

The time-dependent nature of gold solubility is further highlighted in Table 2; for instance, in Oil A at 250 °C, the concentration of dissolved gold increased steadily from 4.6 ppm after 5 days to 19.8 ppm after 30 days. This observation underscores that prolonged interaction between crude oil and gold surfaces promotes enhanced dissolution. Additionally, Oil A, which exhibits the highest sulfur and acid values, demonstrates a much steeper increase in gold solubility with temperature compared to Oils B and C, highlighting the synergistic effect of these properties on the dissolution process. Post-reaction SEM analysis (Fig. 3) supports the solubility trends observed in our experiments. The SEM images reveal extensive surface erosion and numerous dissolution pits on the gold wires that were not present prior to the reaction. The varying dissolution patterns among Oils A, B, and C reflect differences in their respective sulfur and TAN contents, reinforcing the hypothesis that

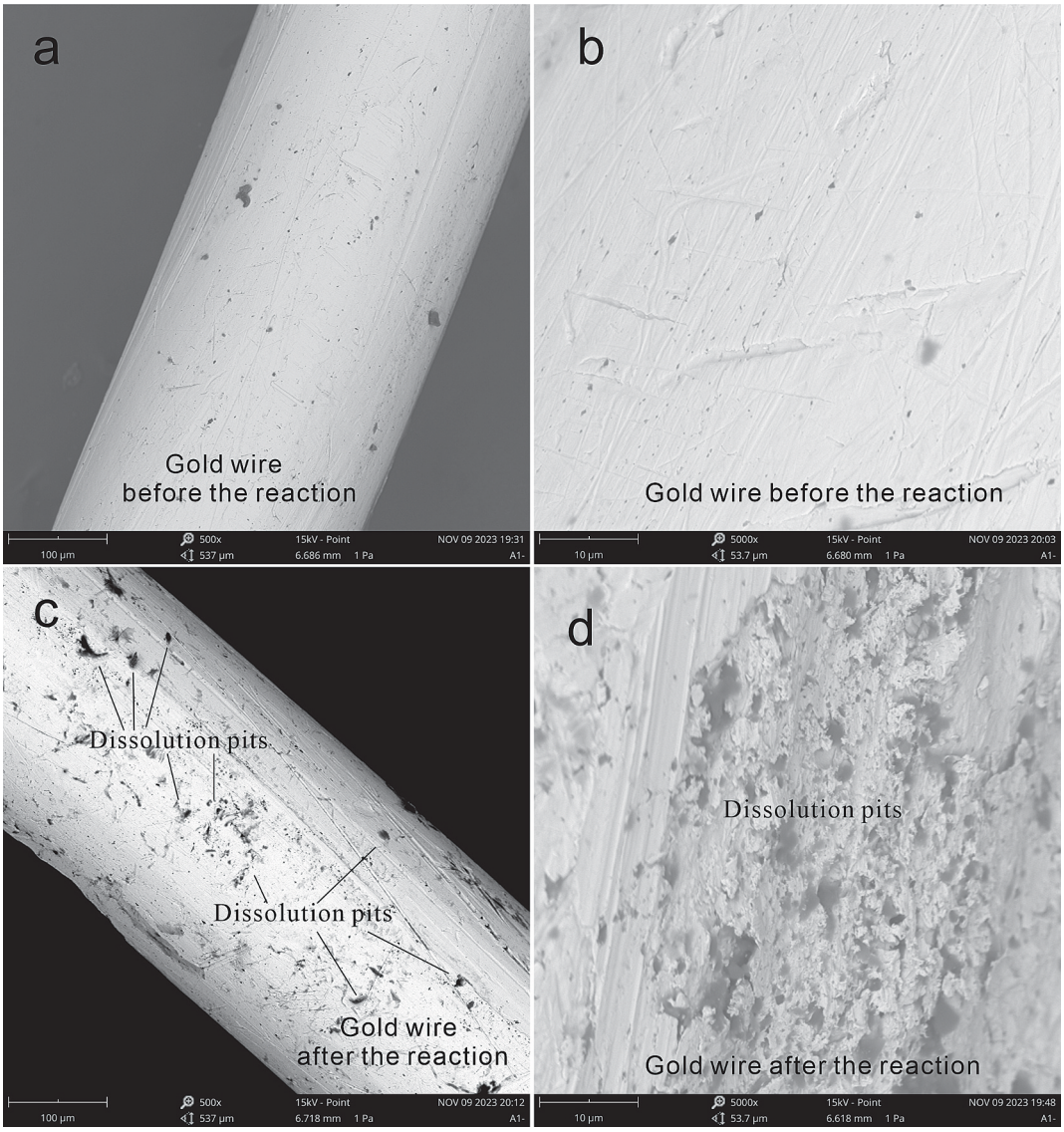

Fig. 3. Scanning Electron Microscope (SEM) images of gold wire: Comparison before and after solubility experiments.

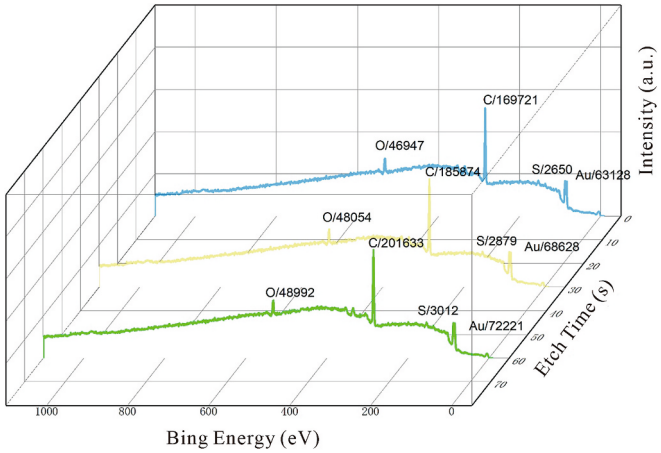

Fig. 4. XPS peak areas of Au, C, O, and S at etching times of 0, 30, and 60 s.

sulfur-driven and acidic mechanisms facilitate gold transport. Furthermore, our XPS results (Fig. 4) show that the peak areas for Au and C increase with etching time (i.e., depth), suggesting a strong association between gold and the organic components in crude oil. The increasing relative oxygen content with depth implies a correlation between gold and oxygen-containing species—most of which exist as carboxylic acids in crude oil (Giordano, 1985). Additionally, the observed increase in sulfur content, with binding energies corresponding to Au–thiolate complexes (160 and 162 eV; Castner et al., 1996; Sanz-Robinson et al., 2020), indicates that a portion of the dissolved gold may be present as Au thiolate complexes. These findings support the view that both sulfur and acidic components are crucial for facilitating gold dissolution, potentially via the formation of thiol or organic acetate complexes (Aleksandrova et al., 2023; Castner et al., 1996; Caumette et al., 2009; Ni et al., 2020; Ni et al., 2024; Sanz-Robinson et al., 2020). However, the thermal stability of these organic ligands at elevated temperatures warrants consideration. Previous studies have shown that thiol compounds can remain stable up to approximately 250 °C under reducing conditions, especially in the absence of oxygen (Crede et al., 2019). Similarly, certain organic acetates have been reported to exist stably at a temperature lower than 300 °C (Ni et al., 2025). Therefore, it is plausible that these complexes could remain intact and actively participate in gold

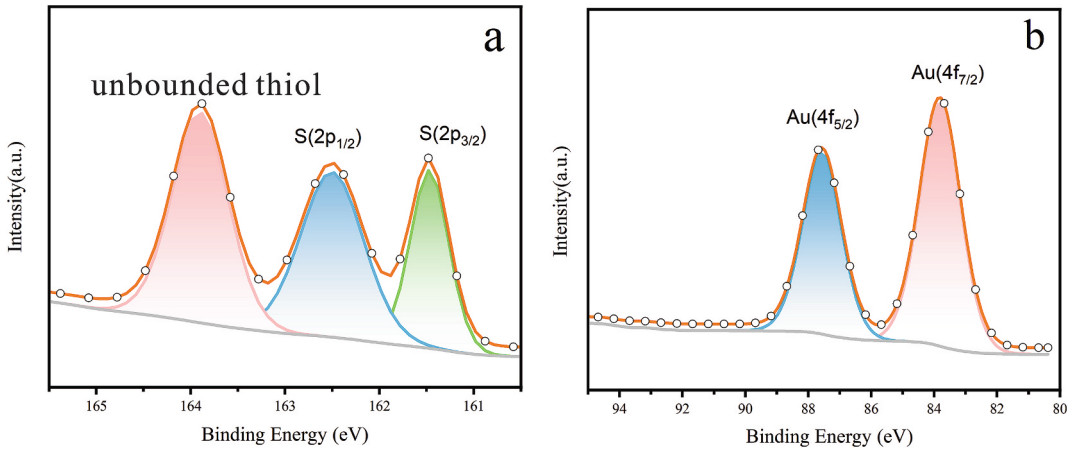

Fig. 5. XPS spectra of Au and thiolate (a) the peak of Au–thiolate complexes; (b).the double peaks of Au (4f5/2 and 4f7/2).

transport within the tested temperature range of 150–250 °C.

An intriguing aspect of our study is that Oil B, despite having the lowest sulfur and TAN values, initially contained the highest gold concentration. This suggests that the native gold content in crude oils is influenced not only by chemical properties such as sulfur or acid content but also by the geological background, including the type of source rock, its thermal maturity, and its mineralization history. Although Oils A and C may derive from less gold-rich source rocks, the unlimited gold provided during our experiments allowed their inherent dissolution capacities to manifest. This observation opens the possibility that gold solubility in crude oil might serve as a tracer for the provenance of gold in petroleum systems.

Overall, our results challenge traditional hydrothermal models of ore genesis by underscoring the role of hydrocarbons as an alternative medium for gold transport in organic-rich and petroleum-bearing systems. The high solubility of gold in sulfur- and acid-rich oils suggests that organic compounds within hydrocarbon reservoirs could significantly contribute to metal concentration and potentially lead to hydrocarbon-driven mineralization processes. With maximum Au concentrations reaching 19.8 ppm at 250 °C—far exceeding the typical 20 ppb observed in conventional hydrothermal fluids (Tu, 1988)—this study opens new avenues for understanding ore-forming processes in organic-rich basins. Future research should aim to identify the specific organic compounds responsible for gold transport and elucidate their interactions with reservoir conditions, which could have important implications for exploration and resource assessment in hydrocarbon-rich regions.

5. Conclusion

This study demonstrates that crude oil, particularly when rich in sulfur and Total Acid Number (TAN), can serve as an effective medium for the dissolution and transport of gold at elevated temperatures. Our results indicate that gold solubility in crude oil increases significantly with both temperature and time, with the highest concentrations observed at 250 °C, especially in oils with higher sulfur and TAN content. The dissolution of gold is likely facilitated by the formation of thiol or organic acetate complexes, which aligns with previous studies suggesting that hydrocarbons can act as solvents for various metals. Post-experiment SEM analysis confirmed significant surface erosion of gold wires, further supporting the hypothesis of gold dissolution in hydrocarbons under high-temperature conditions. These findings challenge traditional models of ore genesis, highlighting the potential role of hydrocarbons in gold mineralization and suggesting that organic-rich fluids could play a more prominent role in the transport of metals across sedimentary basins and petroleum reservoirs. By advancing our understanding of gold behavior in non-aqueous environments, this study opens new avenues for exploring hydrocarbon-driven gold deposits and reassessing ore-forming processes in petroleum-bearing environments.

Declaration of competing interest

The authors declare that they have no known competing financial interests or personal relationships that could have appeared to influence the work reported in this paper.

Acknowledgments

This work was supported by National Natural Science Foundation of China (Grant No. 42273069).

Data availability

No data was used for the research described in the article.

References

Aleksandrova, T., Nikolaeva, N., Kuznetsov, V., 2023. Thermodynamic and experimental substantiation of the possibility of formation and extraction of organometallic compounds as indicators of deep naphthogenesis. Energies 16, 3862.
Anderson, G.M., 2008. The mixing hypothesis and the origin of Mississippi Valley-type ore deposits. Econ. Geol. 103, 1683–1690.
Arehart, G.B., 1996. Characteristics and origin of sediment-hosted gold deposits: a review. Ore Geol. Rev. 11, 383–403.
Broadbent, G.C., Myers, R.E., Wright, J.V., 1998. Geology and origin of shale-hosted Zn-Pb-Ag mineralization at the century deposit, Northwest Queensland, Australia. Econ. Geol. 90, 1264–1294.
Castner, D.G., Hinds, K., Grainger, D.W., 1996. X-ray photoelectron spectroscopy sulfur 2p study of organic thiol and disulfide binding Interactions with gold Surfaces. Langmuir 12, 5083–5086.
Caumette, G., Lienemann, C.-P., Merdrignac, I., Bouyssiere, B., Lobinski, R., 2009. Element speciation analysis of petroleum and related materials. J. Anal. At. Spectrom 24, 263–276.
Chen, Y.J., Ni, P., Fan, H.R., Pirajno, F., Lai, Y., Su, W.C., Zhang, H., 2007. Diagnostic fluid inclusions of different types hydrothermal gold deposits. Acta Petrol. Sin. 23 (9), 2085–2108 (in Chinese with English abstract).
Chen, Y.J., Zhang, J., Liu, C.Q., He, S.H., 2001. The lateral source of the continental oil and gas of China: extension and application of the CPMF model. Geological Rev. 47, 261–271 (in Chinese with English abstract).
Crede, L.S., Liu, W.H., Evans, K.A., Rempel, K.U., Testemale, D., Brugger, J., 2019. Crude oils as ore fluids: an experimental in-situ XAS study of gold partitioning between brine and organic fluid from 25 to 250 °C. Geochim. Cosmochim. Acta 244, 352–365.
Disnar, J.R., Sureau, J.F., 1990. Organic matter in ore genesis: Progress and perspectives. Org Geochem. 16, 577–599.
Drennan, G.R., Robb, L.J., 2006. The nature of hydrocarbons and related fluids in the Witwatersrand Basin, South Africa: their role in metal redistribution. In: Reimold, W. U., Gibson, R.L. (Eds.), Processes on the Early Earth: Geological Society of America Special Paper. Boulder, Colorado, GSA, pp. 353–385.
Emsbo, P., Williams-Jones, A., Koenig, A.E., Wilson, S.A., 2009. Petroleum as an agent of metal transport: metallogenic and exploration implications. Proce. Tenth Biennial SGA Meeting (Townsville) 99–101.

Etminan, H., Hoffmann, C.F., 1989. Biomarkers in fluid inclusions: a new tool in constraining source regimes and its implications for the genesis of Mississippi Valley-type deposits. Geology 17, 19–22.
Fuchs, S., Schumann, D., Martin, R.F., Couillard, M., 2021. The extensive hydrocarbon-mediated fixation of hydrothermal gold in the Witwatersrand Basin, South Africa. Ore Geol. Rev. 138, 104313.
Gaboury, D., 2013. Does gold in orogenic deposits come from pyrite in deeply buried carbon-rich sediments?: Insight from volatiles in fluid inclusions. Geology 41, 1207–1210.
Gaboury, D., 2021. The neglected involvement of organic matter in forming Large and rich hydrothermal orogenic gold deposits. Geosciences 11, 344.
Gibert, F., Pascal, M.L., Pichavant, M., 1998. Gold solubility and speciation in hydrothermal solutions: experimental study of the stability of hydrosulphide complex of gold ($AuHS^0$) at 350 to 450 °C and 500 bars. Geochim. Cosmochim. Acta 62, 2931–2947.
Giordano, T.H., 1985. Evaluation of organic ligands and metal-organic complexing in Mississippi Valley-type ore solutions. Econ. Geol. 80, 96–106.
Giordano, T.H., 1994. Metal transport in ore fluids by organic ligand complexation. In: Pittman, E.D., Lewan, M.D. (Eds.), Organic Acids in Geological Processes. Berlin, Springer, Heidelberg, pp. 270–319.
Goldfarb, R.J., Pitcairn, I., 2023. Orogenic gold: is a genetic association with magmatism realistic? Miner. Deposita 58, 5–35.
Groves, D.I., Santosh, M., Deng, J., Wang, Q.F., Yang, L.Q., Zhang, L., 2020. A holistic model for the origin of orogenic gold deposits and its implications for exploration. Miner. Deposita 55, 275–292.
Groves, D., 1993. The crustal continuum model for late-Archaean lode-gold deposits of the Yilgarn block, Western Australia. Miner. Deposita 28, 366–374.
Gu, X.X., Zhang, Y.M., Li, B.H., Xue, C.J., Dong, S.Y., Fu, S.H., Cheng, W.B., Liu, L., Wu, C.Y., 2010. The coupling relationship between metallization and hydrocarbon accumulation in sedimentary basins. Earth Sci. Front. 17, 83–105.
Hao, F., Zhou, X.H., Zhu, Y.M., Yang, Y.Y., 2011. Lacustrine source rock deposition in response to co-evolution of environments and organisms controlled by tectonic subsidence and climate, Bohai Bay Basin, China. Org Geochem. 42, 323–339.
Helgeson, H.C., Garrels, R.M., 1968. Hydrothermal transport and deposition of gold. Econ. Geol. 63, 622–635.
Herazo, A., Reich, M., Barra, F., Morata, D., Real, I.D., Pagès, A., 2020. Assessing the role of bitumen in the formation of stratabound Cu-(Ag) deposits: insights from the Lorena deposit, las Luces district, northern Chile. Ore Geol. Rev. 124, 103639.
Hu, S.Y., Plet, C., 2022. Introduction to a special issue on organic- and microbe-metal interactions in mineral systems. Ore Geol. Rev. 146, 104938.
Hu, Y.Z., Han, R.S., Mao, X.X., 2007. Relationship between metal mineralization and accumulation of oil and gas in the eastern Guizhou. Geology and Prospecting 43, 51–56.
Hulen, J.B., Collister, J.W., 1999. The oil-bearing, carlin-type gold deposits of Yankee Basin, Alligator Ridge District, Nevada. Econ. Geol. 94, 1029–1049.
Hulen, J.B., Collister, J.W., Stout, B., Curtiss, D.K., Dahdah, N.F., 1998. The exhumed "Carlin-type" fossil oil reservoir at Yankee Basin. JOM 50, 30–34.
Jaraula, C.M.B., Schwark, L., Moreau, X., Pickel, W., Bagas, L., Grice, K., 2015. Radiolytic alteration of biopolymers in the Mulga rock (Australia) uranium deposit. Appl. Geochem. 52, 97–108.
Kerrich, R., Goldfarb, R.J., Richards, J.P., 2005. Metallogenic provinces in an evolving geodynamic framework. Econ. Geol. 100, 1097–1136.
Kesler, S., Jones, H., Furman, F., Sassen, R., Anderson, W., Kyle, J., 1994. Role of crude oil in the genesis of Mississippi Valley-type deposits: evidence from the Cincinnati arch. Geology 22, 609–612.
Li, S.J., Wang, X.C., Hu, S.Y., Guagliardo, P., Kilburn, M., Golding, S.D., Rodrigues, S., Bourdet, J., 2022. Recognition of a widespread Paleoproterozoic hydrothermal system in the southern McArthur Basin, northern Australia, by in-situ analysis of fine-grained pyrite and spatially-associated solid bitumen in the Lamont pass palaeohigh. Ore Geol. Rev. 144, 104834.
Migdisov, A., Guo, X.F., Xu, H.W., Williams-Jones, A., Sun, C.J., Vasyukova, O., Sugiyama, I., Fuchs, S., Pearce, K., Roback, R., 2017. Hydrocarbons as ore fluids. Geochem. Perspect. Lett. 5, 47–52.
Mossman, D.J., 1999. Carbonaceous substances in mineral deposits: implications for geochemical exploration. J. Geochem. Explor. 66, 241–247.
Ni, Z.Y., Zhang, W., Liu, J., Shi, S.B., Wang, X., Su, Y., 2024. Occurrence of state of gold in crude oil and its economic significance. Minerals 14, 351.
Ni, Z.Y., Chen, Y.J., Liu, J., Shi, K., Zheng, H.F., 2025. Study on the thermal persistence of silver acetate: implication for the role of organic acids in metallic mineralization. Ore Geol. Rev. 177, 106450.
Peters, K. E., Walters, C. C., and Moldowan, J. M., 2004. The Biomarker Guide: Volume 2: Biomarkers and Isotopes in Petroleum Systems and Earth History. Cambridge University Press, Cambridge, United Kingdom.
Sanz-Robinson, J., Williams-Jones, A.E., 2019. Zinc solubility, speciation and deposition: a role for liquid hydrocarbons as ore fluids for Mississippi Valley type Zn-Pb deposits. Chem. Geol. 520, 60–68.
Sanz-Robinson, J., Williams-Jones, A.E., 2020. The solubility of nickel (Ni) in crude oil at 150, 200 and 250 °C and its application to ore genesis. Chem. Geol. 533, 119443.
Sanz-Robinson, J., Sugiyama, I., Williams-Jones, A.E., 2020. The solubility of palladium (Pd) in crude oil at 150, 200 and 250°C and its application to ore genesis. Chem. Geol. 531, 119320.
Su, W. C., 2002. Geochemical study of mineralizing fluids in Carlin-type gold deposits at the southwest margin of the Yangtze Block (Doctoral dissertation). Institute of Geochemistry, Chinese Academy of Sciences, Guiyang, China. 60-90.
Su, Y., Sun, X., Ding, Z., 2024. The solubility of antimony (Sb) in liquid Hydrocarbons and its implication for the ore-forming process of orogenic antimony-gold deposits in southern Tibet. Minerals 14, 141.
Sun, Y.Z., Püttmann, W., 2000. The role of organic matter during copper enrichment in Kupferschiefer from the Sangerhausen basin, Germany. Org Geochem. 31, 1143–1161.
Tomkins, A.G., 2013. On the source of orogenic gold. Geology 41, 1255–1256.
Tu, G. Z., 1988. Gechemisty of strata-bound Deposits in China (Volume III). Science Press, Beijing, p. 1-60.
Wang, G.Z., Hu, R.Z., Su, W.C., Zhu, L.M., 2002. Fluid flow and metallogenesis in the Youjiang Basin, Yunnan–Guizhou–Guangxi region, China. Sci. China (Series D) 32, 78–86.
Williams-Jones, A.E., Migdisov, A.A., 2006. An experimental study of the solubility of gold in crude oil: implications for ore genesis. Geochim. Cosmochim. Acta 70, A703.